*[Paleoceanography and Paleoclimatology]*

Supporting Information for

# The δD records of *n*-alkane and *n*-alkanoic acid of tropical trees reflect δD of precipitation during the early stages of the leaf growth

**Amrita Saishree[1], Shreyas Managave[1*], M. G. Yadava[2], Salam Maheshwori Devi[1], Prasanta Sanyal[3]**

[1]Earth and Climate Sciences, Indian Institute of Science Education and Research Pune, Pune 411008, India

[2]Physical Research Laboratory, Navrangpura, Ahmedabad, Gujarat 380 009, India

[3]Department of Earth Sciences, Indian Institute of Science Education and Research Kolkata, Mohanpur 741246, India

* Corresponding author: Shreyas Managave; Email: shreyas@iiserpune.ac.in

## Contents of this file

Text S1 to S6
Figures S1 to S6
Tables S1 to S7

## Additional Supporting Information (Files uploaded separately)

NA

## Introduction

[This document consists of 6 figures, 6 texts and 7 tables.]

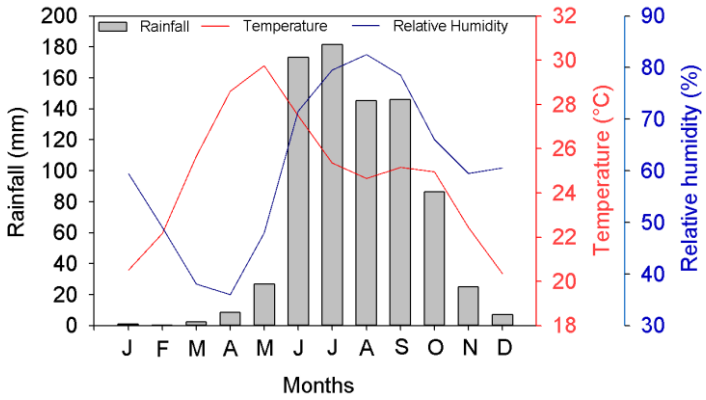


Fig S1. Monthly climatology of rainfall, temperature and relative humidity in the study area. [Data source: India Meteorological Department *Climatological Normals*: (1981 - 2010)]

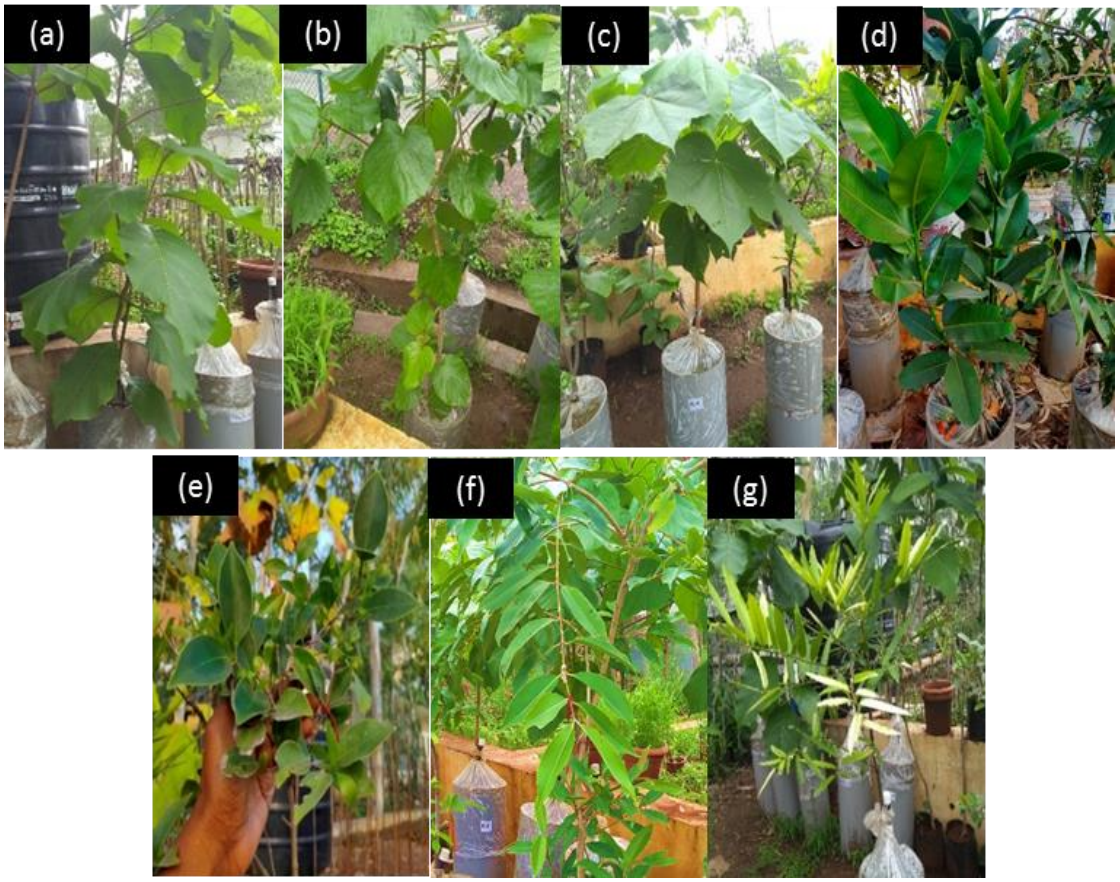


Fig S2. Deciduous [*Tectona grandis* (a), *Haldina cordifolia* (b), *Sterculia urens*(c)] and evergreen [*Callophylum inophyllum* (d), *Memecylon umbellatum* (e), *Syzygium cumini* (f), and *Diospyros malabarica* (g)] species considered in the present study.

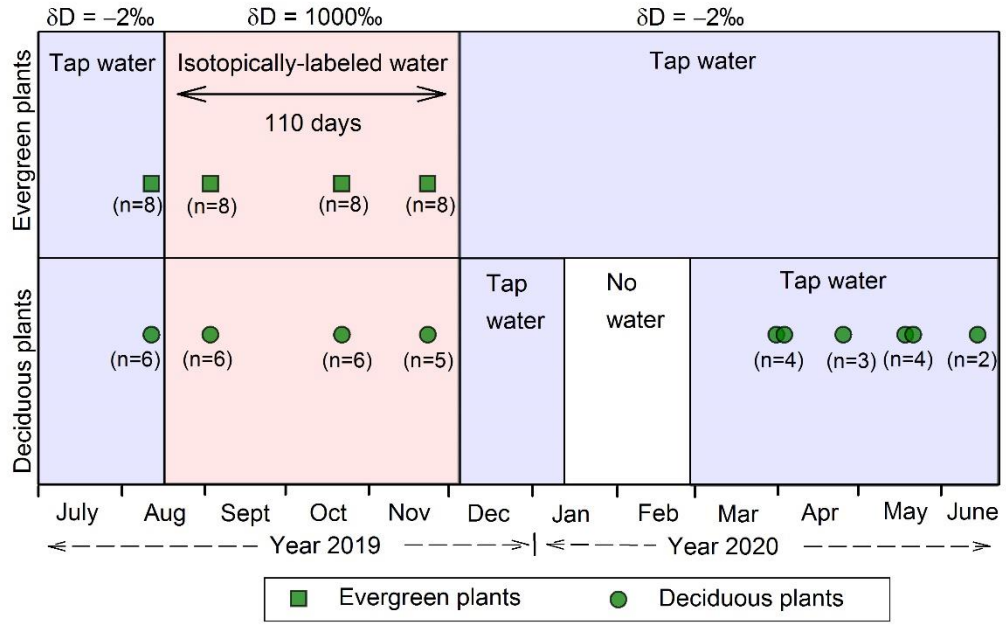


Fig S3. A schematic illustration of the irrigation regime employed and sampling carried out in this study. The purple and beige colors indicate the period of application of normal and tracer water, respectively. After the leafshed, the deciduous species were not irrigated for 47 days (from the 13$^{th}$ of January 2020 to the 29$^{th}$ of February 2020). The squares and circles indicate the day of collection of the leaves; the associated numbers in the parenthesis indicate the number of trees sampled on a given day. In the growing season of 2020, new leaves of only deciduous species were collected.

Fig S4. Pots sealed to prevent the influx of rain. To prevent access to groundwater the pots were kept on the concrete base.

**Text S1: Leaf maturation period**

To identify mature leaves in deciduous species, leaf growth measurement (length measured in one of the fixed dimensions) and leaf mass per unit area (LMA) analysis were carried out (Fig. S5, S6). The isotopically-labeled water was applied after stabilization of the leaf growth (10 to 64 days) and LMA (32 to 82 days). In the case of evergreen species, thicker leaves lying at a lower level on a branch were considered mature and were sampled.

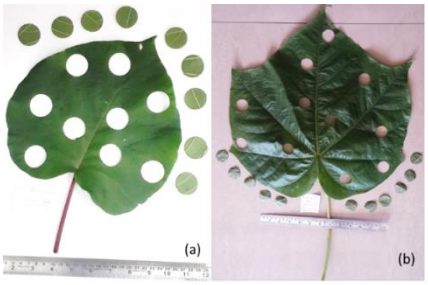


Fig S5. Different parts of leaves were sampled for LMA measurements. For example, (a) *Haldina cordifolia*, and (b) *Sterculia urens*.

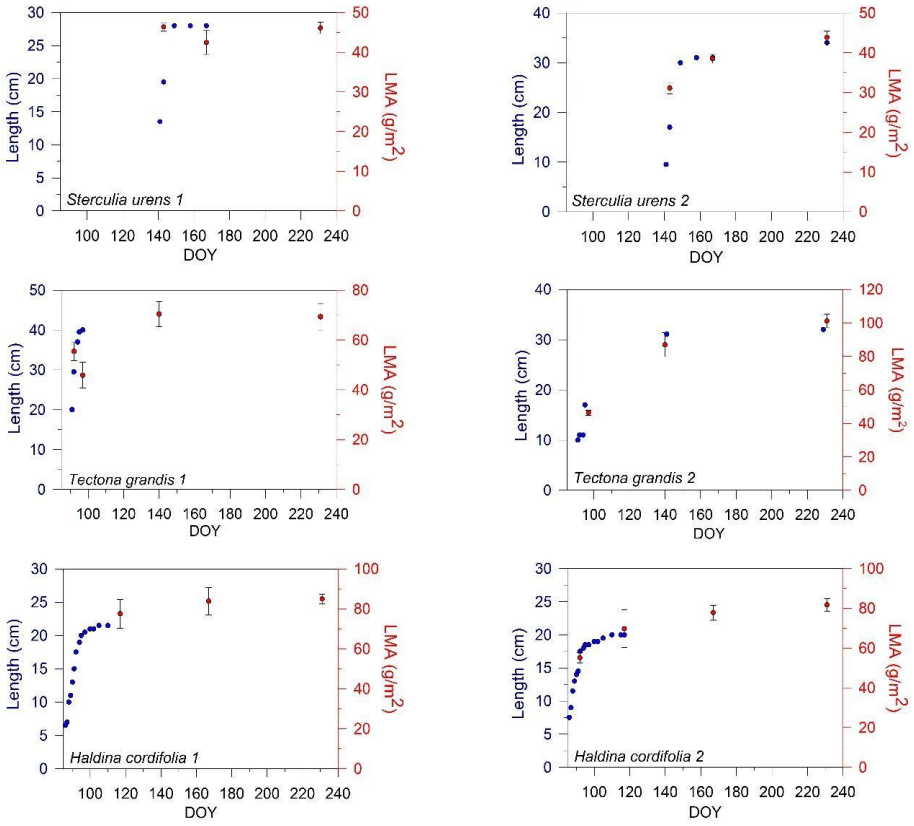


Fig S6. Leaf lengths (blue circles) and LMA (red circles) variation in deciduous leaves.

**Text S2: *n*-alkane and *n*-alkanoic acid extraction**

To obtain the total lipid fraction of the leaf samples, the dried leaves were powdered and ultrasonication technique was followed as described by McInerney et al. (2011). The samples were mixed with a reaction solvent composed of 93:7 v/v dichloromethane/methanol (HPLC grade) and subjected to sonication for 20 minutes at room temperature (25-30°C). The extracted lipid was concentrated using a Rotavapor (R-210; Buchi Labortechnik AG, Flawil, Switzerland). Short-column silica gel chromatography was used to extract *n*-alkane from the total lipid fraction. The column was prepared by using a pre-ashed pipette that was filled with activated silica gel (100-200 mesh), and the non-polar fraction (*n*-alkanes) was separated using hexane as the eluent. Subsequently, a mixture of methanol and dichloromethane in a ratio of 2:1 was utilized to elute the silica gel columns, to obtain the acid fraction. The acids fractions were subjected to saponification using 1 M KOH in methanol at 70 °C for 2 hours. After incubation, the vials were allowed to cool and then 5 % NaCl solution in DCM-extracted HPLC-grade water was added to each vial. The pH of the mixture was lowered (<2) using HCl and the "acids" fractions were extracted using hexane. The "acids" fractions were then extracted using hexane. To perform analysis of *n*-alkanoic acid, the acid fraction was methylated using $BF_3$-methanol and converted into fatty acid methyl esters. Finally, the fatty acid methyl esters were passed through an anhydrous $Na_2SO_4$ column to eliminate any moisture present.

**Text S3: Identification and quantification of leaf wax *n*-alkanes and *n*-alkanoic acids**

Gas chromatography (7890A GC System; Agilent Technologies, Santa Clara, CA, USA) was used to analyze the *n*-alkanes and *n*-alkanoic acids. The system was equipped with split/split-less injector, non-polar capillary column (HP5-MS; 30 m × 250 µm × 0.25 µm), and flame ionization detector (FID). The concentrated samples were injected in 1:1 split mode with an inlet temperature set to 320 °C. The oven temperature was ramped up from 60 °C to 320 °C at a rate of 8 °C minutes$^{-1}$ and held for 12 minutes. The characteristic retention time (RT) obtained from the calibration standards SUPELCO $C_8$-$C_{40}$ alkane and Fluka alkane mixture ($C_{10}$-$C_{40}$) was used to identify individual *n*-alkanes. The relative concentrations of the individual *n*-alkanes in the samples were also calculated using the same standards. To calibrate the system, the SUPELCO $C_8$-$C_{40}$ *n*-alkane standard and Fluka alkane mixture standard ($C_{10}$-$C_{40}$) were measured at different dilutions (1.0 ng, 1.5 ng, and 2.0 ng µl−1) during the analysis of the samples. The peak areas of the individual *n*-alkanes ($C_8$-$C_{40}$ and $C_{10}$-$C_{40}$) were computed, and calibration graphs of peak areas against injected concentration were produced for the respective homologues ($C_8$-$C_{40}$ and $C_{10}$-$C_{40}$). The relative concentration of *n*-alkanes in the samples was then determined using the calibration equations that were obtained from regression analysis for the corresponding homologues. Similarly, the identification of individual *n*-alkanoic acids was achieved through the use of five

Sigma-Aldrich standards: Palmitic-$C_{16}$, Oleic-$C_{18}$, Behenic-$C_{22}$, Montanic-$C_{28}$, and Melissic-$C_{30}$ acid, each with known concentrations. During the analysis of *n*-alkanoic acids, the Fluka *n*-alkane mixture standard ($C_{10}$-$C_{40}$) and SUPELCO $C_8$-$C_{40}$ *n*-alkane standard were also analyzed. Equations for individual *n*-alkanoic acid homologues were derived using *n*-alkanoic acid and *n*-alkane standards. The calibrated equations (for respective homologues) were then used to calculate the relative concentrations of *n*-alkanoic acids in the samples. An uncertainty of ±2% was observed during the repeat measurements of *n*-alkanoic acid and *n*-alkane standards.

**Text S4: the δD measurements**

*Leaf wax n-alkanes and n-alkanoic acids*

The leaf wax *n*-alkanes and *n*-alkanoic acids δD measurements were carried out using the Trace GC Ultra (Thermo Fisher Scientific, Strada Rivoltana 20090 Rodano, Milan, Italy), coupled with a MAT-253 IRMS via a GC Isolink (pyrolysis interface) and Thermo Fisher Scientific Conflo IV interface. A non-polar capillary column HP5-MS was used for sample analysis. The samples were injected in splitless mode, and the inlet temperature was set to 280 °C, with helium used as the carrier gas at a flow rate of 1 ml minutes$^{-1}$. The temperature of the GC oven was set to increase at a rate of 10 °C per minute, starting from 40 °C to 320 °C, held isothermally for 12 minutes. To measure the δD, the hydrogen atoms in the samples underwent conversion to $H_2$ by a reduction interface in a pyrolysis furnace at 1420 °C. To standardize the hydrogen isotope values, $H_2$ reference gas was introduced into MAT-253 in a series of pulses at the beginning and end of each analysis. Before isotope analyses, the $H_2$ reference gas was calibrated against international standard mixtures A7 ($C_{16}$–$C_{30}$). To verify the performance of the instrument, a Fluka alkane mixture ($C_{10}$-$C_{40}$) at various dilutions (ranging from 30 to 100 ng µl−1) was routinely checked with known δD values. The reproducibility of the A7 and Fluka alkane mixture during sample analysis was found to be ±2‰ (1-σ). The $H^{3+}$ factor was calculated using ISODAT NT 3.0 before measurements of hydrogen isotopes. The $H^{3+}$ factor had a range of 7 to 10 ppm nA-1, indicating a contribution of <0.07-0.1% $H^{3+}$ to $HD^+$ (Sarangi et al., 2022). Pre-concentration and dilution procedure were carried out for the chain lengths of excessively low and high concentrations, respectively. Isotope fractionation associated with the addition of $BF_3$-methanol during *n*-alkanoic acid extraction was corrected using a mass balance equation:

$$\delta D_{acid} = \frac{[(2C_n + 2) * \delta D_{FAME}] - [3 * \delta D_{Me}]}{(2C_n - 1)}$$

where, $\delta D_{acid}$ values are the corrected values for target *n*-alkanoic acid, $C_n$ is the number of C-atom for each alkanoic acid chain length, $\delta D_{FAME}$ values are uncorrected values measured from fatty acid methyl esters, and

$\delta D_{Me}$ is the δD value of the methanol in $BF_3$-methanol used to methylate the samples. The δD values of *n*-alkanes and *n*-alkanoic acids are reported with respect to Vienna Standard Mean Ocean Water (VSMOW).

*Water and atmospheric vapor samples*

The tap/tracer water and atmospheric vapor samples were analyzed for δD values at the Physical Research Laboratory (PRL) India, using a laser-based water isotope analyzer (ABB-LGR IWA-45P). The analyzer follows the off-axis integrated cavity output spectroscopy (OA-ICOS) method for the measurement of isotopic composition (Baer et al., 2002). The method introduces laser photons of the known line strength in an optical cavity filled with sample water in vapor form, the measured absorption spectra is recorded and processed by post-analysis software to estimate the isotopic composition. Three standards supplied by ABB-LGR having different δD compositions (std-1: −154 ± 0.5‰, std-2: −51.60 ± 0.5‰, std-3: −9.20 ± 0.5‰) were used in sequence after each batch of 4 water samples during measurements. A protocol 'Standard Natural range optimized for high precision spline type' of measurement was followed. This required 1ml volume of each sample in a standard glass bottle. Using 1μL syringe, samples from these bottles were extracted by an auto-injector system that passed it into a miniature chamber heated at 85°C converting the liquid water fully in vapor form before introducing it into the water isotope analyzer. The δD values are reported with respect to Vienna Standard Mean Ocean Water (VSMOW).

**Text S5: Modeling the δD values of the leaf water during various months**

The Craig-Gordon model, modified by Flanagan and Ehleringer (1991), was used to determine the isotopic enrichment of the leaf water. The following equation was used

$$R_{LW} = \alpha * \left[\alpha_k R_{XW}\left(\frac{e_i - e_s}{e_i}\right) + \alpha_{kb} R_{XW}\left(\frac{e_s - e_a}{e_i}\right) + R_a\left(\frac{e_a}{e_i}\right)\right] \quad \text{(S1)}$$

In equation (1), $R$ is the molar ratio of heavy to light isotope and the subscripts $a$, $LW$ and $XW$ refer to bulk air, leaf water, and xylem water, respectively. α* refers to the liquid-vapor fractionation factor, $\alpha_k$ refers to the kinetic fractionation factor associated with diffusion in air and $\alpha_{kb}$ is the kinetic fractionation factor associated with diffusion at the boundary layer. The default values of $\alpha_k$ and $\alpha_{kb}$ in the model were 1.0164 and 1.011, respectively (Roden et al., 1999). α* varies with leaf temperature (Majoube, 1971). $e_a$, $e_s$ and $e_i$ are the partial pressure of water vapor in bulk air, leaf surface and leaf intercellular air space, respectively. $e_s$ is the only term

that considers leaf physiological characteristics and is calculated using an equation developed by Ball (1987). The values of $e_i$ were estimated from the leaf temperature. Boundary layer conductance was considered as 1 mol $m^{-2}$ $s^{-1}$ (Roden et al., 1999; Managave et al., 2014). Tipple et al., (2015) showed the utility of the Craig-Gordon model in modeling δD values of *n*-alkanes. Due to a lack of leaf parameters such as effective path length, a sophisticated model involving the Péclet effect (Cernusak et al., 2016) was not used. The isotopic composition of the leaf water calculated using Equation 1 is sensitive mainly to (i) leaf temperature, (ii) relative humidity, (iii) isotopic composition of the xylem water (i.e. source water) and atmospheric water vapor (Sachse et al., 2009; Managave, 2014).

Relative humidity data were obtained from a nearby (~1 km) Indian Meteorological Department (IMD) station records while temperature was measured in the field using a thermometer (Table S1). The stomatal conductance was measured using a leaf porometer (Decagon SC-1) (data Table S2). The correlations between the air and leaf temperature for various plants were established using thermistors (Ecomatik LAT-B2) and were used to estimate the leaf temperature and $e_i$. A cryogenic trap method (Deshpande et al., 2013) was used to get an idea about the monthly variability of the δD values of atmospheric water vapor. Table S1 gives the δD of source water and atmospheric water vapor values considered for various months. $R_{LW}$ values are expressed in delta notation for various months (for example for August, $\delta D_{LW}^{Aug*}$).

| Months | Barometric Pressure (KPa)[@] | Temperature (°C)[#] | Humidity (%)[$] | $\delta D_{atm\ vapor}$ (‰)[&] | $\delta D_{source\ water}$ (‰) |
|---|---|---|---|---|---|
| August | 94.4 ± 0.3 | 28.7 ± 2.0 | 82.0 ± 10 | -61 ± 6 | −2 ± 1 |
| September | 94.5 ± 0.3 | 27.1 ± 2.0 | 78.0 ± 10 | -61 ± 6 | 1000 ± 2 |
| October | 94.8 ± 0.3 | 29.6 ± 1.9 | 64.0 ± 12 | -76 ± 8 | 1000 ± 2 |
| November | 95.0 ± 0.3 | 28.1 ± 0.7 | 58.0 ± 9 | -118 ± 12 | 1000 ± 2 |

Table S1. Climate parameters used as inputs for leaf water modeling.

[@] Monthly mean values from IMD station data
[#] Daily measurements from 9 to 12 pm
[$] Daily IMD measurements from 9 to 12 pm; for August it is climatological mean.
[&] Measured periodically. δD values of September were considered for August

| Months | Stomatal conductance (mol $m^{-2}$ $s^{-1}$) | | | | | | |
|---|---|---|---|---|---|---|---|
| | *Tg* | *Hc* | *Su* | *Dm* | *Mu* | *Ci* | *Sc* |
| Aug | 0.5±0.1 | 0.6±0.2 | 0.7±0.3 | 0.4±0.1 | 0.6±0.3 | 0.3±0.1 | 0.5±0.1 |
| Sept | 0.5±0.1 | 0.6±0.2 | 0.7±0.3 | 0.4±0.1 | 0.6±0.3 | 0.3±0.1 | 0.5±0.1 |
| Oct | 0.5±0.1 | 0.7±0.1 | 0.6±0.2 | 0.4±0.04 | 0.6±0.07 | 0.7±0.1 | 0.8±0.5 |
| Nov | 0.4±0.02 | 0.4±0.09 | 0.3±0.08 | 0.3±0.04 | 0.4±0.08 | 0.4±0.09 | 0.6±0.01 |

Table S2. Stomatal conductance used as inputs for the leaf water δD modeling.

***Uncertainty estimation***

The uncertainty associated with different parameters (Table 1) was estimated employing Monte Carlo simulation. These parameters and associated 1-sigma uncertainty were derived from 1000 model runs with simultaneous and random 1-sigma perturbations with the normal distribution of the input parameters given in Table S1 and S2. 10% uncertainty was considered for boundary layer conductance, barometric pressure and the δD value of atmospheric water vapor. Uncertainty in the leaf temperature was the standard error of estimation in the regression of air and leaf temperatures which ranged from 0.5 to 0.9 °C.

| | | *n*-alkanes | | | | *n*-alkanoic acids | | | |
|---|---|---|---|---|---|---|---|---|---|
| | Plants | $\delta D_{alk}^{Aug}$ | $\delta D_{alk}^{Sept}$ | $\delta D_{alk}^{Oct}$ | $\delta D_{alk}^{Nov}$ | $\delta D_{acid}^{Aug}$ | $\delta D_{acid}^{Sept}$ | $\delta D_{acid}^{Oct}$ | $\delta D_{acid}^{Nov}$ |
| Deciduous | *Tg1* | −105 | −117 | −101 | −121 | −106 | −110 | −89 | −125 |
| | *Tg2* | −101 | −102 | −119 | −122 | −101 | −100 | - | −92 |
| | *Hc1* | −93 | −95 | −110 | −64 | −133 | - | −86 | −35 |
| | *Hc2* | −100 | −114 | −121 | −70 | - | −120 | −114 | −54 |
| | *Su1* | −139 | −120 | −111 | - | −157 | −152 | −122 | - |
| | *Su2* | −163 | −109 | −81 | −73 | −158 | −149 | −115 | −92 |
| Evergreen | *Mu1* | −115 | −99 | −92 | −14 | −124 | −134 | −113 | −56 |
| | *Mu2* | −112 | −116 | −111 | −107 | - | −117 | −109 | −89 |
| | *Sc1* | −106 | −115 | −81 | −61 | −91 | −88 | −76 | −92 |
| | *Sc2* | −107 | −109 | −113 | −115 | −103 | −103 | −108 | - |
| | *Ci1* | −149 | −161 | −176 | −145 | −156 | −147 | -189 | -152 |
| | *Ci2* | −148 | −186 | −180 | −166 | −156 | −182 | - | −161 |
| | *Dm1* | −121 | −126 | −126 | 6 | −136 | −134 | −159 | 25 |
| | *Dm2* | −113 | −118 | −120 | −109 | - | −122 | −144 | −139 |

Table S3. Measured δD values of *n*-alkanes and *n*-alkanoic acids in mature leaves of each plant for August, September, October and November. Species abbreviations: *Tg- Tectona grandis, Hc- Haldina cordifolia, Su- Sterculia urens, Mu- Memecylon umbellatum, Sc- Syzygium cumini, Ci- Callophylum inophyllum, and Dm- Diospyros malabarica.*

| Plants | *n*-alkanes | | | | | | *n*-alkanoic acids | | | | | |
|---|---|---|---|---|---|---|---|---|---|---|---|---|
| | $\delta D_{alk}^{Apr}$ | | | $\delta D_{alk}^{May}$ | | $\delta D_{alk}^{June}$ | $\delta D_{acid}^{Apr}$ | | | $\delta D_{acid}^{May}$ | | $\delta D_{acid}^{June}$ |
| | 1st | 4th | 26th | 19th | 22nd | 15th | 1st | 4th | 26th | 19th | 22nd | 15th |
| *Tg1* | - | −42 | - | −59 | - | - | - | −51 | - | −52 | - | - |
| *Tg2* | - | −66 | - | −64 | - | - | - | −68 | - | −68 | - | - |
| *Hc1* | 1 | - | −108 | - | - | - | −19 | - | −37 | - | - | - |
| *Hc2* | - | - | −63 | - | - | −86 | - | - | - | - | - | −72 |
| *Su1* | −50 | - | −107 | - | −132 | - | −64 | - | −113 | - | −138 | - |
| *Su 2* | - | - | - | - | −73 | −112 | - | - | - | - | −88 | −97 |

Table S4. Measured δD values of *n*-alkanes and *n*-alkanoic acids in young leaves of each plant during April, May and June. Species abbreviations: *Tg- Tectona grandis, Hc- Haldina cordifoli, Su- Sterculia urens.*

| | Plants | *n*-alkanes | | | *n*-alkanoic acids | | |
|---|---|---|---|---|---|---|---|
| | | $\delta D_{alk}^{Sept*}$ | $\delta D_{alk}^{Oct*}$ | $\delta D_{alk}^{Nov*}$ | $\delta D_{acid}^{Sept*}$ | $\delta D_{acid}^{Oct*}$ | $\delta D_{acid}^{Nov*}$ |
| Deciduous | *Tg1* | 241±124 | 441±133 | 434±101 | 240±124 | 441±133 | 433±101 |
| | *Tg2* | 241±124 | 446±127 | 441±102 | 241±124 | 446±127 | 441±102 |
| | *Hc1* | 207±118 | 386±133 | 398±105 | 168±118 | 347±133 | 359±105 |
| | *Hc2* | 194±120 | 378±129 | 396±103 | 162±120 | 345±129 | 364±103 |
| | *Su1* | 169±114 | 337±129 | 363±103 | 152±114 | 319±129 | 345±103 |
| | *Su2* | 144±111 | 314±131 | 339±107 | 149±111 | 319±131 | 344±107 |
| Evergreen | *Mu1* | 157±118 | 332±135 | 358±111 | 148±118 | 323±135 | 349±111 |
| | *Mu2* | 160±115 | 337±138 | 356±105 | 148±115 | 325±138 | 345±105 |
| | *Sc1* | 189±113 | 352±132 | 392±102 | 204±113 | 367±132 | 407±102 |
| | *Sc2* | 185±114 | 362±132 | 390±103 | 189±114 | 366±132 | 394±103 |
| | *Ci1* | 146±117 | 322±127 | 342±107 | 139±117 | 316±127 | 335±107 |
| | *Ci2* | 146±114 | 313±127 | 334±111 | 138±114 | 305±127 | 326±111 |
| | *Dm1* | 175±117 | 363±135 | 372±104 | 155±115 | 338±137 | 354±104 |
| | *Dm2* | 187±115 | 348±134 | 383±107 | 152±114 | 338±132 | 349±108 |

Table S5. Modeled δD values of *n*-alkanes and *n*-alkanoic acids in mature leaves of each plant, if the new leaf wax was synthesed using tracer water alone during September, October and November. Species abbreviations as in Table S3.

| | | $\delta D^*_{alk} - \delta D_{alk}$ | | | $\delta D^*_{acid} - \delta D_{acid}$ | | |
|---|---|---|---|---|---|---|---|
| | Plants | Sept | Oct | Nov | Sept | Oct | Nov |
| Deciduous | *Tg1* | 358±124 | 542±133 | 555±101 | 350±124 | 530±133 | 558±101 |
| | *Tg2* | 343±124 | 565±127 | 563±102 | 341±124 | - | 533±102 |
| | *Hc1* | 302±118 | 496±133 | 462±105 | - | 433±133 | 394±105 |
| | *Hc2* | 308±120 | 499±129 | 466±103 | 282±120 | 459±129 | 418±103 |
| | *Su1* | 289±114 | 448±129 | - | 304±114 | 441±129 | - |
| | *Su2* | 253±111 | 395±131 | 412±107 | 298±111 | 434±131 | 436±107 |
| Evergreen | *Mu1* | 256±118 | 424±135 | 372±111 | 282±118 | 436±135 | 405±111 |
| | *Mu2* | 276±115 | 448±138 | 463±105 | 265±115 | 434±138 | 434±105 |
| | *Sc1* | 304±113 | 433±132 | 453±102 | 292±113 | 443±132 | 499±102 |
| | *Sc2* | 294±114 | 475±132 | 505±103 | 292±114 | 474±132 | - |
| | *Ci1* | 307±117 | 498±127 | 487±107 | 286±117 | 505±127 | 487±107 |
| | *Ci2* | 332±114 | 493±127 | 500±111 | 320±114 | 305±127 | 487±111 |
| | *Dm1* | 301±117 | 489±135 | 366±104 | 289±115 | 497±137 | 329±104 |
| | *Dm2* | 305±115 | 468±134 | 492±107 | 274±114 | 482±132 | 488±108 |

Table S6. Differences between the expected and measured δD values of *n*-alkanes and *n*-alkanoic acids for each plant for September, October and November. Species abbreviations as in Table S3.

| | Plants | $f_{new\_alk}$ (%) | | | $f_{new\_acid}$ (%) | | |
|---|---|---|---|---|---|---|---|
| | | Sept | Oct | Nov | Sept | Oct | Nov |
| Deciduous | *Tg1* | −3±1 | 1±1 | −3±1 | −1±1 | 3±1 | −4±1 |
| | *Tg2* | 0±1 | −3±1 | −4±1 | 0±1 | 2±1 | 2±1 |
| | *Hc1* | −1±1 | −4±1 | 6±1 | 4±2 | 10±3 | 20±4 |
| | *Hc2* | −5±2 | −4±1 | 6±1 | 4±2 | 4±1 | 16±3 |
| | *Su1* | 6±2 | 6±2 | 13±3 | 2±1 | 7±2 | 13±3 |
| | *Su2* | 18±6 | 17±5 | 18±4 | 3±1 | 9±3 | 13±3 |
| Evergreen | *Mu1* | 6±3 | 5±2 | 21±5 | −4±2 | 2±1 | 14±3 |
| | *Mu2* | −1±1 | 0±1 | 1±1 | 3±2 | 3±1 | 7±2 |
| | *Sc1* | −3±2 | 5±2 | 9±2 | 1±1 | 3±1 | 0±1 |
| | *Sc2* | −1±1 | −1±1 | −2±1 | 0 | −1±1 | 2±1 |
| | *Ci1* | −4±2 | −6±2 | 1±1 | 3±2 | −7±2 | 1±1 |
| | *Ci2* | −13±5 | −7±2 | −4±1 | −9±4 | −7±2 | −1±1 |
| | *Dm1* | −2±1 | −1±1 | 26±5 | 1±1 | −5±2 | 33±7 |
| | *Dm2* | −2±1 | −2±1 | 1±1 | 5±2 | −2±1 | −1±1 |

Table S7. The estimated fraction of newly synthesized *n*-alkanes ($f_{new\_alk}$) and *n*-alkanoic acids ($f_{new\_acid}$) for September, October and November. Species abbreviations as in Table S3.